Accelerated drop detachment in granular suspensions

Claire Bonnoit, Thibault Bertrand, Eric Clément, and Anke Lindner

Citation: Physics of Fluids **24**, 043304 (2012); doi: 10.1063/1.4704801
View online: http://dx.doi.org/10.1063/1.4704801
View Table of Contents: http://scitation.aip.org/content/aip/journal/pof2/24/4?ver=pdfcov
Published by the AIP Publishing

Accelerated drop detachment in granular suspensions

Claire Bonnoit,[a] Thibault Bertrand,[a),b] Eric Clément, and Anke Lindner
Physique et Mécanique des Milieux Hétérogènes (PMMH), UMR 7636 CNRS, ESPCI, UPMC, Université Paris Diderot, 10, rue Vauquelin, 75231 Paris Cedex 05, France

(Received 3 August 2011; accepted 5 March 2012; published online 27 April 2012)

We experimentally study the detachment of drops of granular suspensions using a density matched model suspension with varying grain volume fraction ($\phi = 15\%$ to 55%) and grain diameter ($d = 20\,\mu$m to $140\,\mu$m). We show that at the beginning of the detachment process, the suspensions behave as an effective fluid. The detachment dynamics in this regime can be entirely described by the shear viscosity of the suspension [R. J. Furbank and J. F. Morris, Int. J. Multiphase Flow **33**(4), 448–468 (2007)]. At later stages of the detachment, the dynamics become independent of the volume fraction and are found to be identical to the dynamics of the interstitial fluid. Surprisingly, visual observation reveals that at this stage, particles are still present in the neck. We suspect rearrangements of particles to locally free the neck of grains, causing the observed dynamics. Close to the final pinch off, the detachment of the suspensions is further accelerated, compared to the dynamics of pure interstitial fluid. This acceleration might be due to the fact that the neck diameter gets of the order of magnitude of the size of the grains and a continuous thinning of the liquid thread is not possible any more. The crossover between the different detachment regimes is a function of the grain size and the initial volume fraction. We characterize the overall acceleration as a function of the grain size and volume fraction. © *2012 American Institute of Physics*. [http://dx.doi.org/10.1063/1.4704801]

I. INTRODUCTION

The stability of jets or the detachment of drops is an important issue in everyday life as well as for industrial applications. The formation of drops can be important for simple liquids, complex fluids, or even dense suspensions or pastes. Especially in the food industry, concentrated suspensions or pastes are processed, extruded from nozzles, or filled in recipients. The formation of drops of particle-laden liquids is of great importance, for instance, for inkjet printing.[1]

The breakup of liquid jets of simple liquids into drops was first described by Plateau[2] and Rayleigh[3] in the 19th century. The final separation of two drops, the so called "pinch off," represents a finite time singularity and has attracted lot of interest lately. Many experimental or theoretical studies report the description of the non-linear behavior of drop separation, reviewed by Eggers.[4]

The fact that the dynamics of the detachment are now well known for simple liquids has also initiated the use of capillary breakup as a rheological technique, allowing to directly access the viscosity of a given fluid.[5] The thinning of the filament, leading to the "pinch off," represents a strong elongation and thus allows to study viscous properties under elongation. Experiments with polymer solutions have shown that this experimental situation is indeed a good set-up to access elongational properties of these fluids.[6–8]

The stability of jets formed by foams, pastes, suspensions, dry grains, or grains immersed in a surrounding liquid has also been addressed.[9–15]

Furbank and Morris[10,11] have studied drop thread dynamics of particle-laden liquids. They have shown that at early stages of the detachment, the suspension can be described as an effective

[a]C. Bonnoit and T. Bertrand contributed equally to this work.
[b]Electronic mail: thibault.bertrand@yale.edu.

fluid. They have also observed that this regime is followed by a second regime, dependent on the characteristics of the individual particles. In this paper, we present a detailed study of the later stages of the detachment process, extending in this way the study of Furbank and Morris[10,11] Comparing to pure oils matching either the shear viscosity of the suspensions[16,17] or the interstitial fluid, we show that the detachment takes place through different regimes. We study the crossover between these regimes as a function of the grain diameter and the volume fraction.[30] We show that the detachment of drops of granular suspensions is accelerated, not only compared to a simple fluid, matching the shear viscosity of the suspensions, but also, at later stages, compared to the dynamics of the interstitial fluid. The overall acceleration is quantified as a function of the volume fraction and the particle diameter.

The paper is organized as follows. In Sec. II, we recall the theory of drop detachment of viscous Newtonian fluids. Section III describes the experimental set-up and the model system. We then introduce the different detachment regimes (Sec. IV) and discuss the transition between these regimes in Sec. V. The acceleration is quantified in Sec. VI and we conclude in Sec. VII.

II. THEORY: DETACHMENT OF A NEWTONIAN FLUID

A pending drop starts to fall, when gravitational forces overcome surface tension. During detachment of the drop, surface tension acts as the main pinching force and tends to thin the filament, linking the drop to the fluid left at the nozzle and gravity becomes negligible. The dynamics of the thinning of the thread are given by a competition between capillarity that tends to thin the filament and viscosity and/or inertia that resist the thinning of the thread.

Such a detachment of a Newtonian fluid can be divided into different regimes. The first regime is governed by linear instability described in the studies on the stability of liquid jets by Plateau[2] and Rayleigh.[3] It corresponds to the instability of a liquid cylinder breaking up into individual drops. The exponential growth of the most unstable mode leads to an exponential evolution of the minimal diameter as a function of time with a given growth rate, depending on the material parameters of the system. In this regime, the evolution of the detachment depends on the initial experimental conditions.

Close to the final detachment, the equations of motion become nonlinear.[4] The "pinch off" is a finite time singularity, localized in space and time. The dynamics thus become independent of the initial conditions or from the particular set-up used. The motion of the fluid can be reduced to a one dimensional problem and the profile of the drop is then governed by universal scaling laws in a self-similar flow.[4,18]

Considering a viscous liquid, Papageorgiou[19] describes theoretically the thinning dynamics of the filament resulting of a competition between capillarity and viscosity, called the Stokes regime. More precisely, the minimum diameter W of the filament (see Figure 2) can be written as

$$W(t) = 2 \times R(t) = 2 \times 0.0708 \times \frac{\gamma}{\eta}(t_{\mathrm{p}} - t), \tag{1}$$

with $R(t)$ the minimum radius of the filament, t_p the time of pinch off, γ the surface tension, and η the viscosity of the fluid.

Close to the pinch off, the radius of curvature tends to zero, leading to an infinite pressure. Then the velocity of the motion diverges and inertia cannot be neglected any more. Eggers[20] gives a theoretical description of this regime of final detachment, called the Navier-Stokes regime, which results in a competition of capillarity, viscosity, and inertia. The minimum diameter W can thus be written as a linear scaling

$$W(t) = 2 \times R(t) = 2 \times 0.0304 \times \frac{\gamma}{\eta}(t_p - t). \tag{2}$$

Experiments have proven the existence of those three different regimes[21,22] for a viscous fluid.

In summary, the drop detachment for a pure viscous fluid takes place via three different regimes, characterized by an exponential regime followed by two linear regimes of different slopes. Usually, one chooses the final pinch off as the reference in time, but strictly speaking, this is relevant only

for the last regime before final detachment and there is no absolute reference on time for the other detachment regimes. This becomes even more important for non-Newtonian fluids, where different detachment dynamics can occur as a function of the nature of the fluid. To be able to compare the dynamics far away from the final pinch, it might be necessary to use another reference in time instead of t_p. This is commonly done, for example, in the study of the detachment of complex fluids[8] and is also what we will do in our analysis.

III. EXPERIMENTAL SET-UP AND MODEL SYSTEM

A. Model suspension and viscous oils

The model suspensions are formed by spherical polystyrene beads from Dynoseeds with different grain diameters $d = 20, 40, 80, 140$ μm and density $\rho = 1050$–1060 kg m^{-3}. The grains almost have a perfect sphericity as guaranteed by the supplier (the ratio of the standard deviation to the mean diameter of the grains is less then 5%). The roughness of the beads has been determined by AFM measurement to be of 100 nm by Deboeuf *et al.* [23] The grains are dispersed in a silicon oil (Shin Etsu SE KF-6011). We measured the viscosity of the pure oil $\eta_0 = 0.18$Pa s and its surface tension $\gamma = 21 \pm 1$ mN m^{-1} at $T = 21^\circ$C. Its density is $\rho = 1070$ kg m^{-3}, as given by the supplier. We vary the volume fraction $\phi = V_g/V_0$ defined as the volume of grains V_g on the total volume V_0 from 15% to 55%. In this way, we prepare monodisperse non-buoyant model suspensions where Brownian motion can be neglected.

In a previous study,[16,17] we have characterized the shear viscosity of this model suspension combining classical and inclined plane rheometry and we have shown that the shear viscosity $\eta(\phi)$ of the suspensions is well described by the Zarraga model[24]

$$\eta_Z(\phi) = \eta_0 \frac{\exp(-2.34\phi)}{(1 - \phi/\phi_m)^3} \tag{3}$$

with $\phi_m = 0.62$ is the maximum packing fraction, close to the random close packing, as obtained by Zarraga *et al.* and η_0 is the viscosity of the interstitial fluid. We use this model to estimate the viscosities of the suspensions used in the present paper (see Figure 1). We also use pure oils AP200 and AP1000 from Sigma Aldrich matching approximately the viscosities of the suspensions of $\phi = 15\%$ and $\phi = 40\%$. Their viscosities measured at $T = 21^\circ$C are given in Table I together with the viscosities of the suspensions. The error in the suspension viscosity is due to an uncertainty of $\pm 1\%$ on the volume fraction. The surface tension of the pure oils is 20 mN m^{-1} at $T = 21^\circ$C.

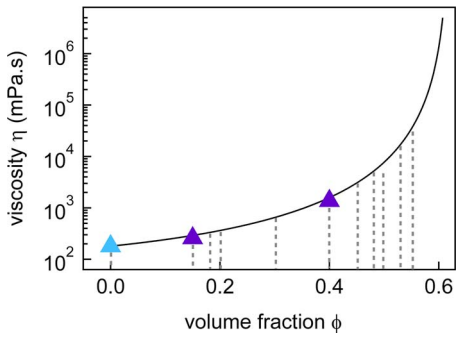

FIG. 1. Viscosities η as a function of the volume fraction ϕ. The solid line represents the prediction by the Zarraga model and the dashed lines indicate the volume fractions of the suspensions used in this study ($\phi = 15\%$, 18%, 20%, 30%, 40%, 45%, 48%, 50%, 53%, and 55%). Triangles represent the pure oils used lighter (cyan online) for the interstitial oil and darker (purple online) for the pure oils approximatively matching the shear viscosity of the suspensions of $\phi = 15\%$ and $\phi = 40\%$).

TABLE I. Table of the viscosities. The viscosities of the suspensions are calculated from the Zarraga model and the viscosities of the pure oils have been measured by classical rheometry. All viscosities are given at 21 °C.

Suspensions	η_{Susp} (Pa s)	Pure oils	η_{PO}(Pas)
		Shin Etsu (η_0)	0.18
$\phi = 15\%$	0.29 ± 0.01	AP200	0.26
$\phi = 40\%$	1.55 ± 0.1	AP1000	1.4

B. Experimental set-up and method

All experiments are performed with the experimental set-up presented in Figure 2. The suspension is filled in a syringe and manually extruded from the latter. The inner diameter of the nozzle is 1.5 mm and the outer diameter is 4 mm. The nozzle is wetted by the fluid and the size of the drop corresponds in the beginning to the outer diameter of the nozzle. The syringe and the camera are mounted on translation stages to place the final detachment in the window of observation of the camera.

A fast camera (Photron Fastcam SA3) records the detachment, with a frame rate of 4000 frames per second at a resolution of 1024 × 256 pixels. We use a macro lens (Sigma 105 mm F 2.8 EX DG) in order to zoom on the drop. Background illumination is provided by a high-brightness

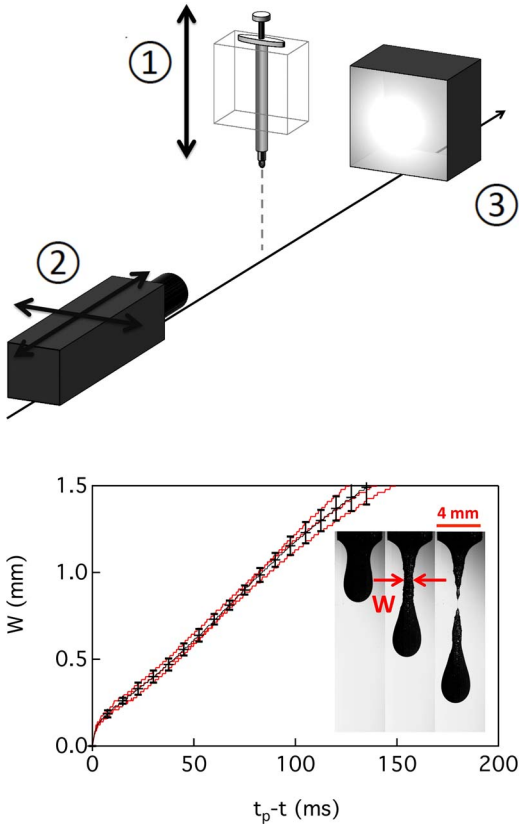

FIG. 2. (Top) Schematic of the experimental set-up. The suspension is extruded from a syringe (1) with an external diameter of 4 mm. The subsequent drop formation is observed via a fast camera (2). Backlight illumination (3) provides high-quality pictures. Arrows indicate the directions of the translational stages. (Bottom) We measure the minimum neck diameter W from the pictures as a function of time t, as can be seen from the inset. The last snapshot represents the moment of final pinch off t_p. The evolution of the neck diameter as a function of $t_p - t$ is shown for three experimental runs for the suspension of $\phi = 15\%$ and $D = 20\,\mu$m. The average and the error bars are shown as well and give an estimate of the reproducibility of our results.

light-emitting diode multihead lamp (300 W), guaranteeing low heat generation, even during prolonged use. In this way, we avoid heating of the drop during detachment. All the experiments presented in this paper where performed at 21°C as measured close to the nozzle. We use a diffuser between the camera and the syringe to get a homogenous illumination of the drop.

For all experiments, we determine the minimal neck diameter W (see Figure 2) as a function of time t during detachment. The moment of final detachment is called t_p and is used as a temporal reference. Image processing with ImageJ is used to extract the profiles of the drops and the minimal neck diameter. We have estimated the resolution of our data to be of 60 μm for the suspensions and of 80 μm for the pure oils. This corresponds to two pixels on the pictures. Data points below this resolution are shown as small gray dotted lines in all graphs representing the time evolution of the neck diameter. The slight difference in resolution is due to the fact that we use a slightly different zoom for the pure oils compared to the suspensions. We conducted three experiments for each condition. The reproducibility of our experiments (see Figure 2 (bottom)) is for the suspensions as well as the pure oils of the order of our spatial resolution for neck diameters smaller than 1.5 mm. Due to the fact that we manually extrude the droplet from the syringe, the data are less reproducible at earlier stages of the detachment process. As we study the detachment close to the final pinch off, this does not influence our measurements. In the graphs showing the time evolution of the experiments, only one experiment is represented per condition, but measurements are always done for three experimental realizations, reflecting in this way the reproducibility.

A first set of experiments is done for a fixed grain size $d = 40$ μm at different volume fractions $\phi = 15\%, 18\%, 30\%, 40\%, 45\%, 48\%, 50\%, 53\%$, and 55%. Up to volume fractions of 55%, no clogging or filtration[25] of the suspension is observed at the outlet of the syringe and the extracted volume fraction is homogeneous and reproducible. A second set of experiments is done for suspensions with four different grain diameters $d = 20$, 40, 80, and 140 μm and two different volume fractions $\phi = 15\%$ and 40%.

The pure oils given in Table I are equally tested. To get insight into the thinning dynamics of the suspensions, we compare the results obtained for the suspensions directly to the results obtained for the pure oils, rather than fitting these results to the predictions for the different detachment regimes given in Sec. II. Our approach has the advantage that we do not need to determine previously in which stage of the detachment process we are and thus allows for an unambiguous discussion of the thinning dynamics of the suspensions.

IV. DIFFERENT DETACHMENT REGIMES

The minimal neck diameter W as a function of $t_p - t$ for the first set of experiments for a grain diameter of $d = 40$ μm and volume fractions from $\phi = 15\%$ to 55% are shown in Figure 3. In addition, the results for the interstitial fluid ($\phi = 0$) are represented. Note that when representing the data as a function of $t_p - t$, the time goes from right to left; from the early stages of the detachment on the right side of the graph to the final pinch off on the left side. At the beginning of the experiment, the evolution of the minimum diameter depends on the initial volume fraction ϕ. One observes that the more concentrated and thus the more viscous the suspensions are, the slower are the dynamics. The thinning of the filament takes longer for the more concentrated suspensions. This is in agreement with observations on viscous oils.[22] At a later stage of the detachment process, all the data collapse onto a single curve. In this regime, the detachment process is independent of the initial volume fraction ϕ and is observed to be identical to the dynamics of the interstitial fluid.

These observations indicate that the detachment takes place via different regimes, the first regime that depends on the volume fraction and the second regime, where the dynamics become independent of the volume fraction and is identical to the dynamics of the interstitial fluid, representing the limit ϕ going to 0.

The results for the interstitial fluid had to be shifted by an offset $\Delta t_{SE} = 20$ ms (see Sec. II) to obtain data collapse with the suspensions onto a single curve. The pinch off for the pure oil is in this representation at $t = -20$ ms, not shown in Figure 3. This indicates that the final detachment for the suspensions is accelerated compared to the interstitial fluid corresponding to a third detachment regime.

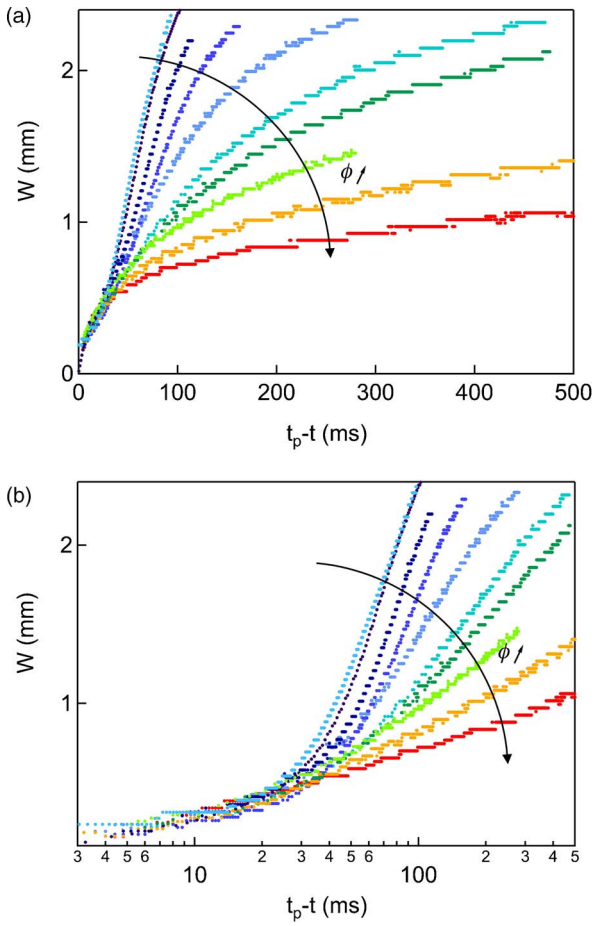

FIG. 3. Time evolution of the minimum neck diameter W for suspensions with volume fractions $\phi = 15\%$, 20%, 30%, 40%, 45%, 48%, 50%, 53%, 55% with grain diameter $d = 40\,\mu$m. The leftmost curve (cyan online) corresponds to the pure interstitial fluid ($\phi = 0$). The origin of the x-axis is given by the time of the pinch for each suspension; the curve for the interstitial fluid is shifted by $\Delta t_{SE} = -20$ ms. (a) lin-lin representation (b) lin-log representation allowing for a better visibility of the short times close to pinch off.

The different regimes can be seen in more detail in Figure 4 (top), where W is represented as a function of $t_p - t$ for a suspension of $d = 140\,\mu$m and $\phi = 40\%$. Results for the pure oil AP1000 matching the effective viscosity of the suspension and the interstitial fluid Shin Etsu are also represented. Note that the curves of the pure oils have been shifted in time, as indicated in the caption of the figure.

From this figure, it is obvious that the first part of the detachment regime corresponds to a regime, where the dynamics are identical to an effective fluid of the corresponding shear viscosity. We will show in the following that this also holds for other grain diameters and volume fractions (Sec. V). The fact that the thinning of the thread is identical for the suspension and the corresponding pure oil shows that there is a regime, where the dynamics in an elongational flow of a granular suspension are solely given by the effective shear viscosity of the suspension. This indicates that the elongational viscosity η_e of model suspensions is solely given by the shear viscosity η, as for Newtonian fluids, where $\eta_e = 3\eta$. This observation is in agreement with the results by Furbank and Morris[11] obtained using a different method. These results are also in agreement with results by Clasen *et al.*[26] on colloidal suspensions, showing that the elongational viscosity is solely given by the shear viscosity. Recent findings by Miskin and Jaeger[27] also confirm this observation and point out the importance of the presence of grains for the later stages of the detachment process.

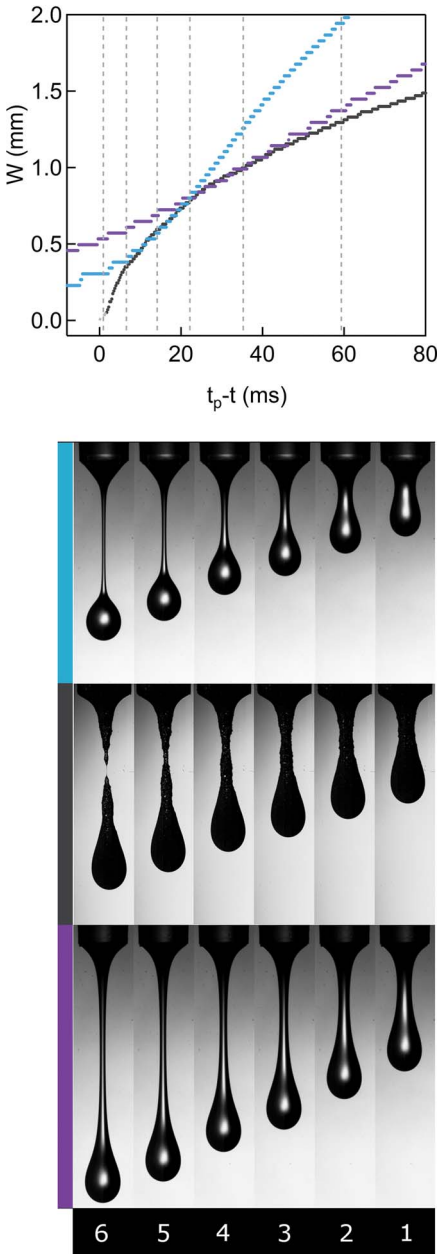

FIG. 4. (Top) Evolution of the minimal neck diameter W for a suspensions with $d = 140$ μm and $\phi = 40\%$ (gray) for the pure interstitial oil Shin Etsu (lighter – cyan online) and for the pure oil AP1000 (darker – purple online) matching the shear viscosity of the suspension. The origin of the x-axis is given by the time of the pinch off for the suspension; the graphs for the pure oils Shin Etsu and AP1000 are shifted $\Delta t_{SE} = -30.75$ ms and $\Delta t_{AP_{1000}} = -124$ ms, respectively. (Bottom) Corresponding snapshots for the interstitial oil Shin Etsu (Top), the suspension (Middle), and the pure oil AP1000 (Bottom). The snapshots are taken at the moments of the detachment process indicated by the dashed lines and are discussed in the text.

At a certain neck diameter, one observes the crossover to the regime where the thinning dynamics are identical to the interstitial fluid. And finally, the suspensions detach more quickly than the interstitial fluid.

In summary, we observe three different detachment regimes: I) a regime where the dynamics are governed by the shear viscosity of the suspensions and the suspensions behave as an effective fluid; II) a regime where the dynamics are given by the interstitial fluid, and III) a final detachment regime close to the final pinch off.

Figure 4 (bottom) shows snapshots of these different regimes for the suspension and the two pure oils at the moments of the detachment process are indicated by the dashed lines in the figure. On the first two snapshots (1 and 2), one observes the thinning of the neck in the effective fluid regime. The neck radius is identical between the pure oil AP1000 and the suspension. The third snapshot shows the transition toward the interstitial fluid regime. No obvious change in the form of the drops can be observed at this stage. Surprisingly, one observes from these pictures that in the interstitial fluid regime (picture 4), there are still grains present in the neck. Roughness appears on the surface of the drop of granular suspension in this regime. In the last two pictures (5 and 6), one observes the crossover to the final detachment regime for the suspension. The suspension detaches very quickly compared to the drop of interstitial fluid that shows a slow thinning of a stable long viscous thread. It can be seen from these pictures that the deformation of the neck becomes very localized for the suspension and that the volume of the suspension that is actually deformed is reduced in this regime.

V. CROSSOVER BETWEEN DIFFERENT REGIMES

In the following, we discuss the crossover between the three different detachment regimes. To do so, we focus on two selected volume fractions: $\phi = 15\%$ and 40% and vary the grain diameter from $d = 20\,\mu$m to $d = 140\,\mu$m.

A. Crossover from effective fluid to interstitial fluid regime

Figure 5 (top) represents the minimal neck diameter for suspensions of different grain diameter and $\phi = 15\%$ together with the pure oil AP200 and $\phi = 40\%$ together with the pure oil AP1000, respectively. The results for the suspensions have been shifted such as to obtain the best agreement with the pure oils. The values for the corresponding offsets in time Δt are given in the caption. For both the volume fractions, one observes clearly that in a certain range of W, we obtain very good agreement between the thinning dynamics of the suspensions and the pure oils. This shows once again that at early stages of the detachment process, the dynamics are governed by the shear viscosity and the suspensions behave as an effective fluid. For neck diameters smaller than a given value of W, the neck thins more quickly for the suspensions than for the pure oil. This change in dynamics takes place at different values of the neck diameter that we call W_{eff} and is a function of the grain diameter d. From the graphs, one observes that for larger d this change in dynamics occurs at larger W_{eff}.

We have measured W_{eff} for the three runs conducted for each experimental condition. To determine W_{eff}, we use as a criterion that the curves for the minimal neck diameter between the suspensions and the pure oil differ by more than our experimental resolution. In Figure 6, W_{eff} is represented as a function of the grain diameter d for the two volume fractions. W_{eff} is typically of the order of 10 grains. The crossover to the interstitial fluid regime takes place at earlier stages of the detachment process (and thus at larger W_{eff}) for larger grain diameters. The increase in W_{eff} with d is observed to be less than linear. For higher volume fraction, deviations from the effective fluid regime take place at larger neck diameters.

The snapshots shown in Figure 5 (bottom) show pictures around the transition toward the interstitial fluid regime for $d = 80\,\mu$m. They will be discussed in more detail in Subsection V C.

B. Crossover from the interstitial fluid to the final detachment regime

Analogous to the study of the transition from the effective to the interstitial fluid regime, we have studied the transition from the interstitial fluid regime to the final detachment regime. Figure 7 (top) shows the results for suspensions of different grain diameters of volume fraction $\phi = 15\%$ and $\phi = 40\%$ together with the interstitial fluid Shin Etsu. From these figures, one can observe that there is a regime where the thinning dynamics are indeed identical for the suspensions and the interstitial fluid. One can also note that for the different grain diameters, this regime can occur at very different neck radii and the thinning of the suspension and the interstitial fluid regime can be identical either during the exponential decay or during the linear regime corresponding to the Papageourgiou regime

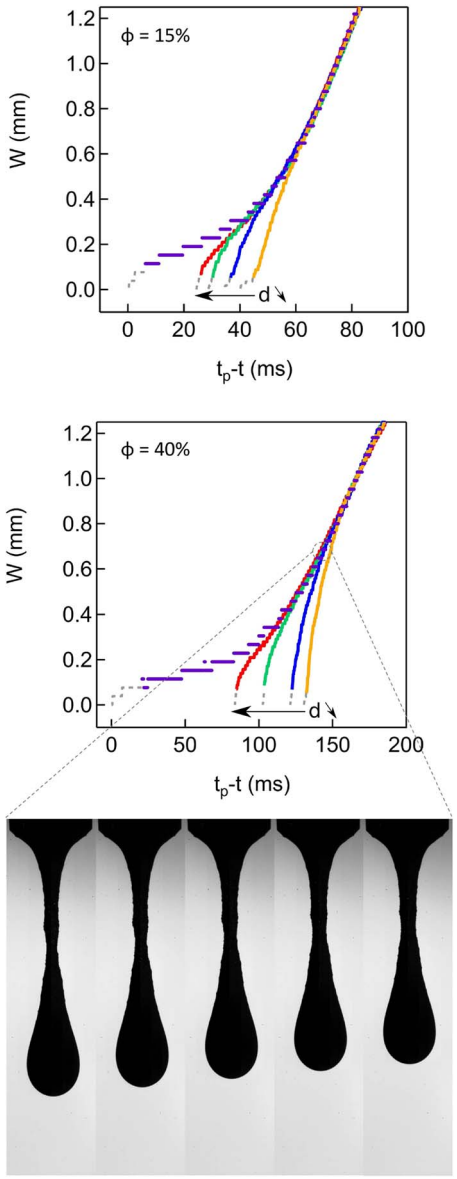

FIG. 5. (Top) Thinning dynamics for suspensions close to the deviation from the effective fluid regime for particle diameters of 20 μm (red online), 40 μm (green online), 80 μm (blue online), and 140 μm (orange online) (from left to right) for volume fractions of $\phi = 15\%$ and $\phi = 40\%$. The (dashed – purple online) curves represent the pure oils matching the shear viscosities of the suspensions, AP200 and AP1000, respectively. The origin of the x-axis is given by the time of the pinch off for the pure oils, the curves for the suspensions have been shifted to match the effective fluid regime ($\phi = 15\%$: $\Delta t_{20} = 24.50$ ms, $\Delta t_{40} = 28.75$ ms, $\Delta t_{80} = 34.50$ ms and $\Delta t_{140} = 40.25$ ms. $\phi = 40\%$: $\Delta t_{20} = 83.75$ ms, $\Delta t_{40} = 102.75$ ms, $\Delta t_{80} = 121.25$ ms and $\Delta t_{140} = 130.50$ ms). (Bottom) Snapshots for suspensions of $d = 80$ μm particles for $\phi = 40\%$ at the transition. The time interval between two snapshots corresponds to $\Delta t = 2.5$ ms.

(see Sec. II). From these figures, it is also obvious that the final detachment of the suspensions is accelerated compared to the pure interstitial fluid.

We have measured the neck radius W_{int} at which the thinning dynamics start to differ between the suspensions and the interstitial fluid. In Figure 8, W_{int} is represented as a function of the grain diameter d. For larger grains, the crossover to the final detachment regime takes place earlier in the detachment process compared to smaller grains. Typically, the crossover to the accelerated detachment regime takes place at a neck diameter that corresponds to some grain diameters. Once

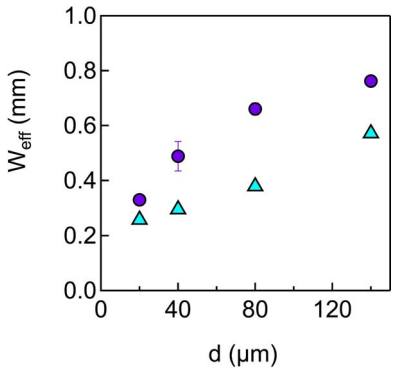

FIG. 6. Average neck diameter at the transition between the effective fluid and the interstitial fluid regime as a function of grain size for $\phi = 15\%$ (△ – cyan online) and $\phi = 40\%$ (◯ – purple online). Some of the error bars are not visible as they are smaller than the symbol size.

again the dependence of W_{int} on d is weak and the increase of W_{int} with d is observed to be less than linear. The crossover does not seem to depend on the volume fraction.

C. Discussion

In the first two paragraphs of this section (Secs. V A and V B), we have shown that the three detachment regimes introduced in Sec. IV are identical for different volume fractions and grain diameters. The crossover between the different regimes however is a function of the volume fraction and the grain diameter. In this paragraph, we discuss the visual observations from Figures 4, 5, and 7 and give possible interpretations of the origin of the mechanisms responsible for the different detachment regimes.

The snapshots in Figure 5 show images taken around the transition between the effective fluid regime and the interstitial fluid regime for a volume fraction of $\phi = 40\%$ and $d = 80\ \mu$m. First of all, one does not observe an obvious change in the visual appearance of the drops close to the transition. It is also clear that grains are still present in the neck at the transition. One observes that the drop seems to get rougher close to the transition to the interstitial fluid regime. Note that this roughness is not on the scale of individual particles, but corresponds rather to aggregates of several particles. Royer *et al.*[15] have recently observed similar formation of aggregates during the destabilization of a dry granular jet. In our case, rearrangements of the particles locally free space of grains in the neck of the suspension and the thinning of the thread becomes more localized. Localized thinning has also been observed during detachment of drops of cornstarch.[28] In our case, this might be at the origin of the fact that the detachment process becomes independent of the volume fraction and is identical to the interstitial fluid, even if visual observations reveal that grains are still present in the neck.

In Figure 7, snapshots close to the crossover to the final detachment regime are shown. In this regime, the neck diameter becomes of the order of magnitude of the grain size (few grain diameters). During the final detachment regime, the deformation of the thread becomes very localized and the thinning does not seem to be a continuous process any more. The volume deformed in the neck does not evolve continuously, but decreases by steps. In this way, the presence of grains prevents the formation of a long, stable filament.

We have recently discussed the evolution of the drop shape during the detachment in more detail in Bertrand *et al.*[29]

VI. ACCELERATION

Figure 9 shows W as a function of $t_p - t$ for $\phi = 15\%$ and $\phi = 40\%$ and different grain diameters together with the results for the pure oils AP200 and AP1000. All results are represented

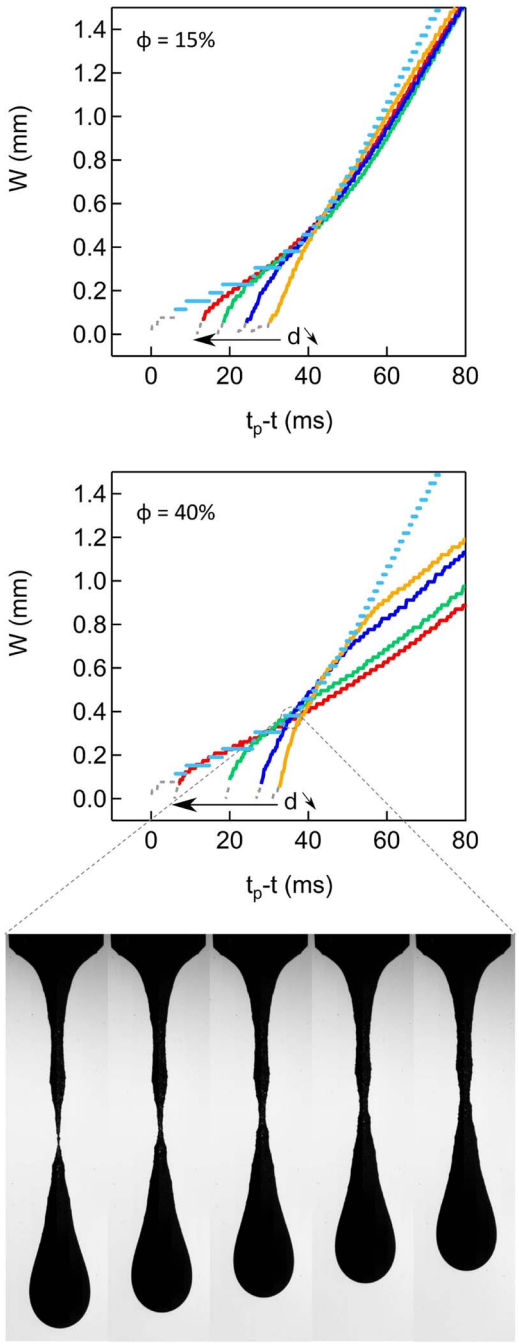

FIG. 7. Thinning dynamics for suspensions close to the deviation from the interstitial fluid regime for particle diameters of 20 μm (red online), 40 μm (green online), 80 μm (blue online), and 140 μm (orange online) (from left to right) for a volume fraction of: $\phi = 15\%$ and $\phi = 40\%$. The (dashed – cyan online) curves represent the interstitial fluid. The origin of the x-axis is given by the time of the pinch off for the interstitial fluid; suspension curves have been shifted to match the interstitial fluid regime ($\phi = 15\%$: $\Delta t_{20} = 11.75$ ms, $\Delta t_{40} = 17$ ms, $\Delta t_{80} = 22$ ms, and $\Delta t_{140} = 25.5$ ms; $\phi = 40\%$: $\Delta t_{20} = 5$ ms, $\Delta t_{40} = 19$ ms, $\Delta t_{80} = 26.75$ ms, and $\Delta t_{140} = 31$ ms). (Bottom) Snapshots for suspensions of $d = 80$ μm particles for $\phi = 40\%$ at the transition. The time interval between two snapshots corresponds to $\Delta t = 2.5$ ms.

with respect to their real pinch off time. In this representation, one observes that the suspensions detach significantly faster than the pure oils matching the shear viscosity of the suspensions. We have quantified this effect by measuring the ΔT at $W = 1$ mm between the suspensions and the corresponding pure oils, as shown in Figure 9. Note that at $W = 1$ mm, all suspensions are in the

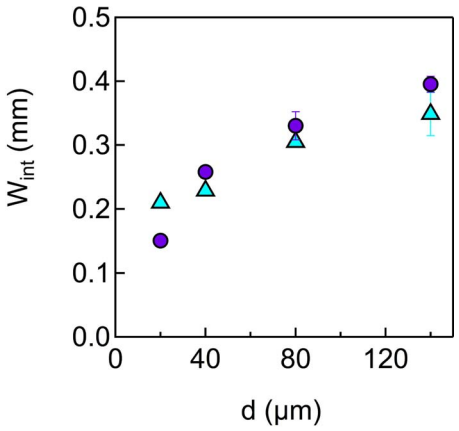

FIG. 8. Average neck diameter at the transition between the interstitial fluid and the final detachment regime as a function of grain size for $\phi = 15\%$ ($\triangle$ – cyan online) and $\phi = 40\%$ ($\bigcirc$ – purple online). Some of the error bars are not visible as they are smaller than the symbol size.

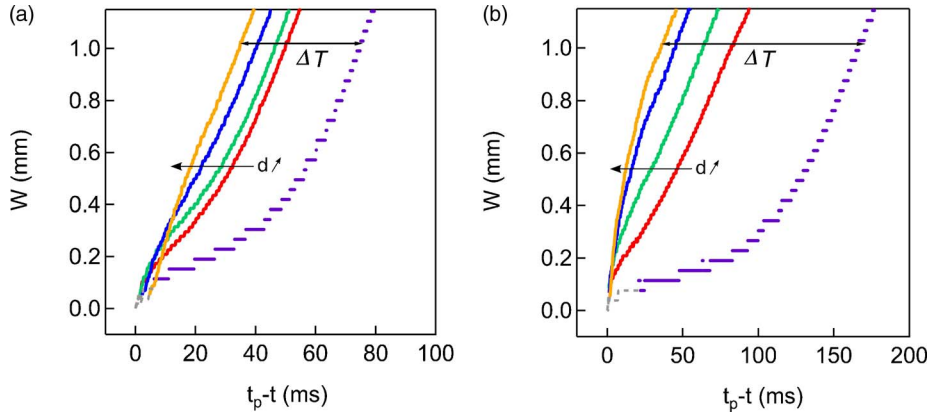

FIG. 9. Characterization of the acceleration during the drop detachment process for different grain sizes: 20 μm (red online), 40 μm (green), 80 μm (blue), 140 μm (orange) (from right to left) for volume fraction of (a) $\phi = 15\%$ and (b) $\phi = 40\%$. The respective pure oils are represented by a dashed line.

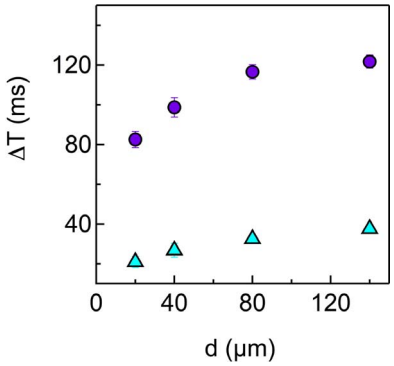

FIG. 10. Average difference in rupture time ΔT between the suspensions and the pure oils as a function of the particle diameter for $\phi = 15\%$ ($\triangle$ – cyan online) and $\phi = 40\%$ ($\bigcirc$ – purple online). Some of the error bars are not visible as they are smaller then the symbol size.

effective fluid regime and their dynamics are at this stage identical to the dynamics of the pure oils. ΔT thus quantifies the acceleration of the detachment due to the presence of particles in the thread.

Figure 10 shows ΔT as a function of the grain diameter d for the two different volume fractions. In both cases, one observes that the difference in rupture time is a function of the grain diameter d.

The difference between the pure oil and the suspensions is more pronounced for the higher volume fraction than for the smaller volume fraction. This is due to the fact that the overall acceleration has two origins. First in the interstitial fluid regime, the dynamics are given by the viscosity of the interstitial fluid η_0. The fact that η_0 is smaller than the shear viscosity of the suspensions leads to an acceleration of the detachment process. This acceleration is more important for the higher volume fractions as the difference in viscosity is higher for the latter. Then, the final detachment is accelerated for the suspensions compared to the interstitial fluid. The transitions in between these two regimes are a function of the grain diameter. The total acceleration is thus a function of the volume fraction and the grain diameter.

VII. CONCLUSION

In this paper, we have shown that the detachment of a drop of dense granular suspension takes place through a number of different regimes.

In the beginning of the detachment, the suspensions behave as an effective fluid and the dynamics of the detachment process are identical to those observed for pure oil of the same shear viscosity. This indicates that the elongational viscosity of a granular suspension is solely given by the shear viscosity, as it is the case for a Newtonian fluid. At a certain stage of the detachment, the drop enters a different detachment regime. The thinning dynamics in this regime are found to be independent of the initial volume fraction and is identical to the dynamics of the pure interstitial fluid. The dynamics of the detachment of the suspensions thus correspond to the dynamics of a fluid without grains. Visual observations reveal however that grains are still present in the neck at this stage. We suspect rearrangements of grains to lead to density fluctuations in the neck, which becomes locally free of grains. These regions have a significantly lower viscosity compared to the suspensions and they thus dominate the thinning dynamics. The deviation from the effective fluid regime is a function of the grain diameter and the volume fraction. Higher volume fractions and higher grain diameter lead to a deviation from the effective fluid regime at earlier stages of the detachment process, and thus at a larger neck diameter. This neck diameter is found to be of the order of 10 grain diameters, but is not linearly proportional to the latter.

The interstitial fluid regime is followed by a final detachment regime for the suspensions. The presence of grains in the neck prevents the formation of a stable and long filament, as is observed for pure interstitial fluids. At the crossover to this regime, the thinning becomes very localized and the thinning of the filament does not seem to be a continuous process any more. In other words, the volume that is deformed is reduced. The deviation from the interstitial fluid regime is given by the grain diameter. It occurs typically at a neck radius of about 3 grain diameters, but it is once again not linearly proportional to the latter.

The fact that the detachment of a granular suspension takes place via these three different regimes leads to an overall acceleration of the detachment process compared to pure oil matching the shear viscosity of the suspensions. This acceleration is a function of the volume fraction and the grain diameter. It is more important for the higher volume fractions and the higher grain diameters. For larger grain diameters, the crossover to the interstitial fluid regime and the accelerated regime takes place at earlier stages of the detachment, leading to a stronger acceleration. For the higher volume fractions, the difference in viscosity between the interstitial fluid and the suspension is larger, leading also to a stronger difference between the detachment dynamics between the effective fluid and the interstitial fluid regime.

In summary, we have shown that the detachment of granular suspensions takes place via three different detachment regimes. We have characterized the crossover among these different regimes as a function of the volume fraction and the grain diameter. The detachment of the suspensions is accelerated compared to a pure fluid matching the shear viscosity of the suspensions. This acceleration is also a function of the volume fraction and the grain diameter.

ACKNOWLEDGMENTS

We acknowledge interesting discussions with Jens Eggers, Christian Clasen, Daniel Bonn, Hamid Kellay, Christian Wagner, Alexander Morozov, Mark Miskin, and Heinrich Jaeger.

[1] N. F. Morrison and O. G. Harlen, "Viscoelasticity in inkjet printing," Rheol. Acta **49**, 619 (2010).
[2] J. Plateau, *Statique Expérimentale et Théorique des Liquides Soumis aux Seules Forces Moléculaires* (Gauthier-Villars, Paris, 1873).
[3] Lord Rayleigh, "On the capillary phenomena of jets," Proc. R. Soc. London **29**, 71 (1879).
[4] J. Eggers, "Nonlinear dynamics and breakup of free-surface flows," Rev. Mod. Phys. **69**(3), 865–929 (1997).
[5] G. H. McKinley and A. Tripathi, "How to extract the newtonian viscosity from capillary breakup measurements in a filament rheometer," J. Rheol. **44**(3), 653–670 (2000).
[6] Y. Amarouchene, D. Bonn, J. Meunier, and H. Kellay, "Inhibition of the finite-time singularity during droplet fission of a polymeric fluid," Phys. Rev. Lett. **86**(16), 3558–3561 (2001).
[7] R. Sattler, C. Wagner, and J. Eggers, "Blistering pattern and formation of nanofibers in capillary thinning of polymer solutions," Phys. Rev. Lett. **100**(16), 164502 (2008).
[8] V. Tirtaatmadja, G. H. McKinley, and J. J. Cooper-White, "Drop formation and breakup of low viscosity elastic fluids: Effects of molecular weight and concentration," Phys. Fluids **18**(4), 043101 (2006).
[9] P. Coussot and F. Gaulard, "Gravity flow instability of viscoplastic materials: The ketchup drip," Phys. Rev. E **72**(3), 031409 (2005).
[10] R. J. Furbank and J. F. Morris, "An experimental study of particle effects on drop formation," Phys. Fluids **16**(5), 1777–1790 (2004).
[11] R. J. Furbank and J. F. Morris, "Pendant drop thread dynamics of particle-laden liquids," Int. J. Multiphase Flow **33**(4), 448–468 (2007).
[12] R. Lespiat, R. Höhler, A. L. Biance, and S. Cohen-Addad, "Experimental study of foam jets," Phys. Fluids **22**(3), 033302 (2010).
[13] D. Lohse, R. Bergmann, R. Mikkelsen, C. Zeilstra, D. van der Meer, M. Versluis, K. van der Weele, M. van der Hoef, and H. Kuipers, "Impact on soft sand: Void collapse and jet formation," Phys. Rev. Lett. **93**(19), 198003 (2004).
[14] F. Pignatel, M. Nicolas, E. Guazzelli, and D. Saintillan, "Falling jets of particles in viscous fluids," Phys. Fluids **21**(12), 123303 (2009).
[15] J. R. Royer, D. J. Evans, L. Oyarte, Q. Guo, E. Kapit, M. E. Mobius, S. R. Waitukaitis, and H. M. Jaeger, "High-speed tracking of rupture and clustering in freely falling granular streams," Nature (London) **459**(7250), 1110–1113 (2009).
[16] C. Bonnoit, J. Lanuza, E. Clement, and A. Lindner, "Inclined plane rheometry of a dense granular suspension," J. Rheol. **54**, 65–79 (2010).
[17] C. Bonnoit, J. Lanuza, A. Lindner, and E. Clement, "A mesoscopic length scale controls the rheology of dense suspensions," Phys. Rev. Lett. **105**, 108302 (2010).
[18] D. H. Peregrine, G. Shoker, and A. Symon, "The bifurcation of liquid bridges," J. Fluid Mech. **212**, 25–39 (1990).
[19] D. T. Papageorgiou, "Analytical description of the breakup of liquid jets," J. Fluid Mech. **301**, 109–132 (1995).
[20] J. Eggers, "Universal pinching of 3d axisymmetrical free-surface flow," Phys. Rev. Lett. **71**(21), 3458–3460 (1993).
[21] T. A. Kowalewski, "On the separation of droplets from a liquid jet," Fluid Dynamics Res. **17**(3), 121–145 (1996).
[22] A. Rothert, R. Richter, and I. Rehberg, "Formation of a drop: Viscosity dependence of three flow regimes," New J. Phys. **5**, 59 (2003).
[23] A. Deboeuf, G. Gauthier, J. Martin, Y. Yurkovetsky, and J. F. Morris, "Particle pressure in a sheared suspension: A bridge from osmosis to granular dilatancy," Phys. Rev. Lett. **102**(10), 108301 (2009).
[24] I. E. Zarraga, D. A. Hill, and D. T. Leighton, "The characterization of the total stress of concentrated suspensions of noncolloidal spheres in newtonian fluids," J. Rheol. **44**(2), 185–220 (2000).
[25] S. D. Kulkarni, B. Metzger, and J. F. Morris, "Particle-pressure-induced self-filtration in concentrated suspensions," Phys. Rev. E **82**(1), 010402 (2010).
[26] C. Clasen, private communication, 2010.
[27] M. Z. Miskin and H. M. Jaeger, "Droplet formation and scaling in dense suspensions," PNAS **109**(12), 4389–4394 (2012).
[28] M. Roché, H. Kellay, and H. A. Stone, "Heterogeneity and the role of normal stresses during the extensional thinning of non-Brownian shear-thickening fluids," Phys. Rev. Lett. **107**, 134503 (2011).
[29] T. Bertrand, C. Bonnoit, E. Clement, and A. Lindner, "Dynamics of drop formation in granular suspensions: The role of the volume fraction," Granular Matter (to be published), doi:10.1007/s10035-012-0318-3.
[30] C. Bonnoit, "Ecoulement de suspensions granulaires modèles", Ph.D. thesis, Université de Paris 6, 2009.